



A long-term in situ calibration system for chemistry analysis of seawater*

Chun-yang TAN^{†1}, Bo JIN^{†‡1}, Kang DING², William E. SEYFRIED Jr.², Ying CHEN¹

(¹State Key Lab of Fluid Power Transmission and Control, Zhejiang University, Hangzhou 310027, China)

(²Department of Geology and Geophysics, University of Minnesota, Minneapolis 55455, USA)

[†]E-mail: cytan@yahoo.cn; bjin@zju.edu.cn

Received Oct. 26, 2009; Revision accepted Mar. 15, 2010; Crosschecked Aug. 11, 2010

Abstract: An in situ calibration system is a versatile exploration instrument for electrochemical sensors investigating the biochemical properties of the marine environment. The purpose of this paper is to describe the design of an auto-calibrating system for electrochemical (pH) sensors, which permits two-point in situ calibration, suitable for long-term measurement in deep sea aqueous environments. Holding multiple sensors, the instrument is designed to perform long-term measurements and in situ calibrations at abyssal depth (up to 4000 m). The instrument is composed of a compact fluid control system which is pressure-equilibrated and designed for deep-sea operation. In situ calibration capability plays a key role in the quality and reproducibility of the data. This paper focuses on methods for extending the lifetime of the instrument, considering the fluidics design, mechanical design, and low-power consumption of the electronics controller. The instrument can last 46 d under normal operating conditions, fulfilling the need for long-term operation. Data concerning pH measured during the KNOX18RR cruise (Mid-Atlantic Ridge, July-August, 2008) illustrate the desirable properties of the instrument. Combined with different electrodes (pH, H₂, H₂S, etc.), it should be of great utility for the study of deep ocean environments, including water column and diffuse-flow hydrothermal fluids.

Key words: pH, Long-term, In situ calibration, Flow control, Low power

doi: 10.1631/jzus.A0900643

Document code: A

CLC number: TH766

1 Introduction

Over the last decade, numerous efforts have focused on the development of instrument technology in chemical oceanography, since the determination and monitoring of key chemical parameters is crucial to the study of the physical and biochemical characteristics of the oceans. For example, pH is expected to be a crucial parameter in deep sea studies: a decrease in pH could have large-scale impacts on marine

ecosystems (Orr *et al.*, 2005). The pH of surface seawater has already decreased by 0.1 units and will continue to decrease by 0.2–0.3 units over the next century as a consequence of the anthropogenic CO₂ absorbed by the oceans (Orr *et al.*, 2005). Accordingly, long-term monitoring of seawater pH may provide insight into global climate change (Chen *et al.*, 2006). In situ measurement technologies, which greatly improve spatial and temporal resolution, are of particular interest to marine scientists (Ding *et al.*, 2005; Ding and Seyfried, 2007).

Subsequently, a variety of electrochemical sensors have been developed successfully for deep sea application, due to their simplicity and low cost, such as those sensors for pH, H₂, H₂S and S²⁻ (Reimers and Glud, 2000). The standard glass electrode is most often used for pH measurement. For example, the commercial pH sensors (AMT Inc., Germany; Sea

[‡] Corresponding author

^{*} Project supported by National Natural Science Foundation of China (No. 40637037), the National High-Tech Research and Development Program (863) of China (No. 2007AA091901), the National Science Foundation of U.S. (No. 0525907), and the China Scholarship Council (No. 2009632124)

© Zhejiang University and Springer-Verlag Berlin Heidelberg 2010

Bird Inc., USA, etc.) and custom-designed pH sensors (Le Bris *et al.*, 2001; 2003) utilize a typical glass electrode for pH measurement in seawater and hydrothermal diffuse fluids. Recent progress with metal oxide electrodes composed of iridium has shown significant potential for application to pH measurement at elevated temperatures and pressures (Pan and Seyfried, 2008). Despite the abundance of data obtained by existing technologies, inaccuracies still exist owing to liquid junction potentials in seawater (Dickson, 1993a; 1993b), these inaccuracies being as high as ± 0.1 pH units (Le Bris *et al.*, 2005). This greatly reduces their effectiveness for benthic applications. Conversion to pH still relies on laboratory calibrations (Le Bris *et al.*, 2001). For long-term applications, signal drift and poor instability at high pressure are caused by irreversible compositional change to the surface phase of the electrodes over time, after which the electrode requires in situ calibration. Therefore, lack of in situ calibration and maintenance greatly influences the lifetime of pH sensors for deep sea applications.

Consequently, we have designed and constructed an auto-calibrating system for electrochemical (pH) sensors, the design of which permits two-point in situ calibration, suitable for long-term measurement in deep sea aqueous environments. The electrodes are cleaned and maintained during the calibration process. In this paper, we focus on the proposed method to reduce the energy loss in the instrument design and the low-power consumption of the electronics in order to extend the lifetime of the auto-calibrating system for in situ observation.

2 Mechanism design

To perform in situ measurement, sensors must make contact with the sample, and interact with two different standards to conduct the calibration. This means there is a requisite displacement of one fluid by another during the process. To meet this functional requirement, the instrument was designed as a compact flow control system which includes two components: a flow control unit and a sensor head (Fig. 1). The piston pump inside the flow control unit continuously delivers the fluids into the flow cell. Valves V1–V3 are utilized to select the seawater sample or

standard (e.g., buffer solutions). The sensor unit is sealed inside the flow cell to interact with the fluids. The inlet port of valve V1 is exposed to the seawater while the inlet ports of valves V2 and V3 are connected to flexible bags containing standard pH buffer solutions. The fluid-controlling components run at ambient hydrostatic pressure in the silicone oil-filled chamber. An oil-filled rubber reservoir is used to compensate the silicone oil in the flow control chamber. The flow cell is positioned in the sensor head in such a way that the sample is drawn through the sensors, instead of being pushed, to minimize the dead volume. During the pH measurement process, the pump unit draws the water sample through valve V1 into the flow cell. In situ calibration is accomplished by drawing the buffer solutions, in sequence, to flush the flow cell and rinse the electrodes.

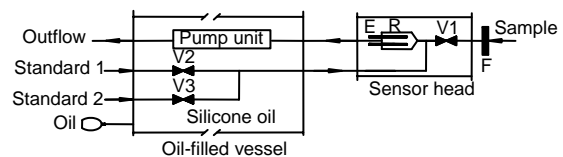


Fig. 1 Schematic illustrations of the flow through system V1–V3: solenoid diagram valves (normal close); E: electrodes; R: reaction cell; F: filter

This electrohydraulic system is an open loop system in which there is no hydraulic actuator and the input power is only used to deliver the fluids through pipes. In this system the main energy loss h_f can be described as

$$h_f = \sum h_l + \sum h_m, \quad (1)$$

where h_l is the friction loss in the pipes and can be described as

$$h_l = \lambda \frac{l U^2}{d 2g}, \quad (2)$$

where λ is the resistance factor of the pipes, l is the length of pipes, U is the flow velocity, and d is the inner diameter of the pipes.

h_m is the local energy loss caused by the valves and disturbance of the flow, such as the geometry modification of the pipes, and can be described as

$$h_m = \frac{Q^2}{Av^2g} + \xi \frac{U^2}{2g}, \quad (3)$$

where Q is the flow rate, Av is the valve capacity coefficient, and ξ is the local resistance factor. So Eq. (1) can be expressed as

$$h_f = \sum \lambda \frac{l}{d} \frac{U^2}{2g} + \sum \frac{Q^2}{Av^2g} + \sum \xi \frac{U^2}{2g}. \quad (4)$$

Eq. (4) shows that there are several factors for energy loss, such as the length of the pipes, the flow rate and the systematic scheme design of the hydraulic system.

The flow control unit (Fig. 2) utilizes a plastic housing (80 mm in I.D., 300 mm in length) to contain the flow control components. To reduce the energy loss (Eq. (4)), solenoid valves (LVM05R6A, SMC Inc., Japan) are mounted on a custom engineered polycarbonate manifold, which reduces space and weight. It also reduces the piping required. The valves are modified to assure that the solenoid assembly is oil-immersed, which permits pressure equilibration. From Eq. (4), the pressure loss was calculated to be about 59.2 kPa. To balance reliability and energy efficiency, a piston pump (LPVX0504950B, Lee Inc., USA) was used during construction of the pump unit. The electronics connected the flow control unit with a water resistant cable, which is protected by a custom made plastic chamber. The inside volume of the flow control unit is filled with silicone oil for water resistance at great depth. A rubber reservoir filled with oil is connected to the inside volume through the manifold for hydrostatic pressure balance between the inside and outside of the chamber.

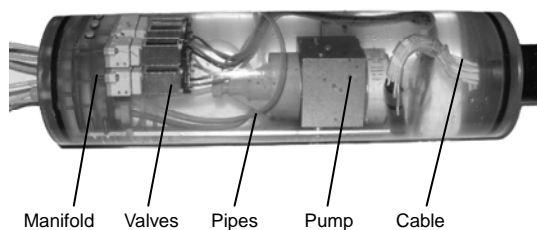


Fig. 2 A photograph of the flow control unit

During calibration, one fluid in the reaction cell needs to be displaced by the successive fluid. The

faster this displacement process works, the less energy is used. The reaction cell was designed to have an internal volume of only 1.03 ml, despite containing five electrodes. The displacement process was tested on land at atmosphere pressure to validate the reaction cell and to optimize the sequence of deep sea timed operations. In this test, artificial seawater and buffer solutions were prepared according to a standard procedure using deionized water and reagent grade solid chemicals (Fisher Scientific, USA). Each solution contained 0.57 kg/mol NaCl in keeping with the dissolved chloride concentration of seawater. pH of the seawater was measured to be 8.25; pH (25 °C) of buffer 1 and buffer 2 was 7.00 and 10.37, respectively, determined by Ross pH electrode. First, the seawater was drawn into the flow cell through valve V1. The second and third steps (replacement of one fluid by another) involved a calibration operation in which buffer 1 and buffer 2 were drawn into the flow cell sequentially. The flow rate was 7.5 ml/min and each step was set to be 20 min. The potential of the electrodes was simultaneously measured and recorded by the data-logger, with sampling rates of twenty measurements per minute. The results are shown in Fig. 3. When pH was changed, the measured potential revealed immediate response, and the curve of each step was characterized by an asymptotic approach to a stable reading at each pH condition. Generally 5 min were required to achieve steady-state conditions, that is, the absolute displacement of one fluid by another in the reaction cell.

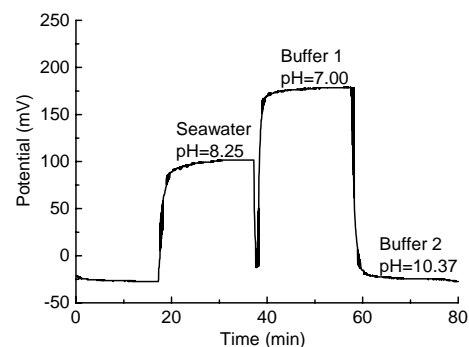


Fig. 3 Measured cell potential during on-board test at 27.8 °C. These data reveal generally good correspondence in the pH-mV data

The auto-calibrating system has three pressure housings, with an ability to resist water pressure to

70 MPa. They are made of titanium alloy due to its high strength, low density, and resistance to corrosion. One housing (114 mm in diameter, 276 mm in length) contains the electronics for system control, another (130 mm in diameter, 482 mm in length) contains a battery for the power supply (12 V), and the third housing (84 mm in diameter, 260 mm in length) contains a data-logger for the signal processing and data storage of the sensor unit.

The auto-calibrating system is designed to perform time series and long-term (more than one month) observations, thereby providing a reliable tool for multidisciplinary benthic research down to depths of 4000 m. Laboratory research has proven the feasibility of the system to calibrate the electrode (Fig. 3). Pressure testing in a high pressure vessel showed that the electronics and fluid control system operated well at pressures up to 40 MPa.

3 Low-power electronics design

Power consumption is a main concern in electronic circuit and system design for oceanographic engineering. A high degree of power consumption causes shorter battery life, increases the mean-time-between-failure (MTBF) and decreases reliability of the circuits (Kumar *et al.*, 2004). To facilitate deployment, this device was designed to be a self-contained unit, which includes a reliable power supply and an electronics system for control and data processing. The duration of undersea performance is restricted by battery life, which is related to the power consumption of the electronics. System-level dynamic power management (DPM) was used in the electronics design of the system. DPM achieves energy-efficient computation by selectively placing the system components into low power modes when they are idle (or partially utilized) (Benini *et al.*, 2000; 2001). State mode transitions are controlled by commands issued by a power manager (PM) that observes the workload of the system and, in effect, determines when and how to force power mode transitions. DPM strategy was used while switching operating frequency and varying the supply power of the components under performance constraints to minimize power consumption according to a power management strategy (Chen *et al.*, 2003).

3.1 Power-management systems

The electronic controller of the instrument is a set of interacting components (units) and is designed to meet the following requirements: (1) the lowest power consumption; (2) real-time management capacity of the fluid-controlling components; (3) high data storage capacity to accommodate the data produced by the instrument; (4) high communication capability.

The hardware organization is shown in Fig. 4. The MSP430 microcontroller was the micro controller unit (MCU), used due to its low power consumption and robust on-chip peripheral modules, such as 12-bit analog/digital (A/D), which can greatly simplify the circuit design. The TB6560 stepping motor driver is used for the step motor driving application, receiving PWM signals from MCU timer. A high capacity flash memory (33-megabit AT45DB321C) was selected to store the periodical data during the mission. The data includes the time stamp, the status of the fluid-controlling components, and the voltage of the battery, which can be collected on board after retrieval. Two communication channels are provided by the communication module, one channel is RS232 interfaced for large quantity data from the flash memory, and the other is an inductively coupled link (ICL) that allows instrument control via non-contact serial communication with the submersible (Bradley *et al.*, 1995). A 12-V NiMH battery pack (13.5 Ah) has been selected for the power supply. To protect the instrument and battery pack, the electronics controller is equipped with a battery status sensor to monitor the battery voltage for the purpose of shutting down the whole system at a particular state of charge (SOC).

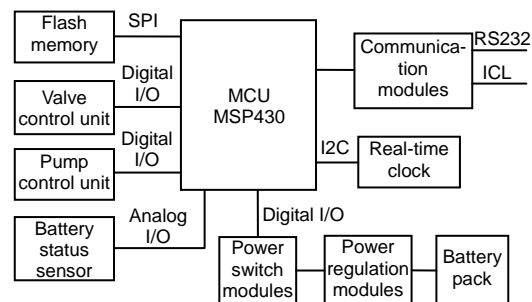


Fig. 4 Hardware diagram of electronic controller

To implement the DPM, the electronic controller is designed to be a power-managed system, in which all major components, i.e., the MCU, flash memory, communication module, real-time clock, valve control unit, pump control unit, and battery status sensor are power-manageable and can be put into a low-power sleep mode. The MCU has two clock resources: a 32768-Hz watch crystal oscillator for low-power mode operation and an internal digitally-controlled oscillator (DCO) for the active mode (Zhao *et al.*, 2009). Power regulation is based on a set of low quiescent current linear regulators, while the dedicated power switch modules allow the mission management software to switch on (working mode) or off (idle mode) each major component according to the preprogrammed strategy or the occurrence of significant events (failures, energy loss, etc.). Significant differences can be found in the energy budget of power managed components (PMC) between the working mode and idle mode, which underscores the need for DPM strategy (Table 1).

Table 1 Power budget of power managed components

Power managed component	Power budget		
	Supply voltage (V)	Average working current (mA)	Idle current (μA)
Flash memory	3.3	10	6
Real-time clock	3.3	0.8	0.25
Communication modules (ICL)	9	7.5 ^{rx} , 50 ^{tx}	500
Battery status sensor	12	1.1	70
Valve driving unit	12	240	50
Pump driving unit	12	400	50

rx: receive; tx: transmit

3.2 Dynamic power management implementation

In most cases, power management for the electronic controller is based on a hybrid hardware-software implementation. For the flexibility of DPM implementation, PM is migrated by the software. The core power management functionality is implemented as the program operating in the MCU. The MCU is usually in the low power sleep mode and waits for interrupt requests (IRQ) to activate the unit. All sub-routines (A/D conversion, communication, etc.) of the software program are designed as interrupt service routines (ISR). IRQs are generated by the internal timer and external real-time clock PCF8563.

In general, DPM policies target the maximization of battery life by controlling the system operation mode or its components. Power-managed systems must be able to operate in different states, which compromise performance for power consumption (Benini *et al.*, 2001). Table 2 enumerates the components power modes corresponding to four useful states, characterized by increasing power consumption. These states are based on actual working conditions and the PM works for the state transition according to the formulated policy. Communication modules are only active during deployment: testing on board and data transition are not taken into account. In seawater, the auto-calibrating platform works in two actual modes. In idle mode, PM puts the MCU and all the PMCs into low power mode to save power (S0). However, the PM signals a wake up to the electronics every 60 s to sample and record the main parameters of the instrument in the flash memory (S1). The duration of the sampling and flash memory writing is 125 ms. Under working conditions, the instrument performs measurements periodically and then returns to the sleep state S0. If calibration is needed, the instrument performs the calibration cycle to standardize and clean the sensors (S2). Power consumption for measurement and calibration is exactly the same. During this process, the sample process is still carried out every 60 s (S3). The average current of the idle condition (I_{Idle}) and the average current of the working condition (I_{Working}) are given by the relationship as follows:

$$I_{\text{Idle}} = \frac{(60 - T_{S1}) \times I_{S0} + T_{S1} \times I_{S1}}{60}, \quad (5)$$

$$I_{\text{Working}} = \frac{(60 - T_{S3}) \times I_{S2} + T_{S3} \times I_{S3}}{60}, \quad (6)$$

where I_{S0} , I_{S1} , I_{S2} , and I_{S3} are the average currents of each state (Table 2), while T_{S0} , T_{S1} , T_{S2} , and T_{S3} are the durations of each state. I_{Idle} is calculated to be 5.025 mA and I_{Working} is 700.025 mA. Without DPM implementation, I_{Idle} and I_{Working} are measured to be 12 and 770 mA, respectively. The lifetime t of the battery can be calibrated by

$$t = \frac{C_{\text{battery}}}{I_{\text{Idle}} \times t_{\text{Idle}} + I_{\text{Working}} \times t_{\text{Working}}}, \quad (7)$$

where C_{battery} is the capacity of the battery, t_{idle} and t_{working} are the idle duration and working duration during one period, respectively.

Table 2 Useful states for electronic controller

Power managed component	State			
	S0	S1	S2	S3
MCU	Sleep	On	On	On
Flash memory	Idle	On	Idle	On
Real-time clock	Idle	On	Idle	On
Battery status sensor	Idle	On	Idle	On
Valve control unit	Idle	Idle	On	On
Pump control unit	Idle	Idle	On	On
Current (mA)	5	17	700	712

3.3 Power estimation

For the auto-calibrating system, the most critical issue is battery lifetime. To predict and optimize battery runtime and circuit performance undersea, we utilized a battery model (Chen and Rincón-Mora, 2006) to simulate the dynamic behavior of the battery pack in PSpice software (Fig. 5). The detailed extraction method of the parameters in the model is described by Schweighofer *et al.* (2003). To verify the accuracy of extraction results, these parameters were applied to the proposed model in PSpice environment to simulate the battery voltage response to the pulse discharge current of 700 mA. Fig. 6 shows that the simulation result and the experimental data are in close agreement. The model regenerates voltage response with less than 0.7% error which manifests the accuracy of parameter extraction.

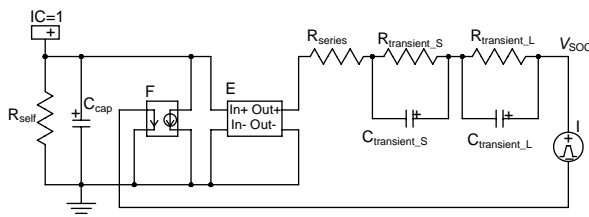


Fig. 5 Battery model for power estimation

R_{self} : self-discharge resistor; C_{cap} : full-capacity capacitor; F: current control current source; E: voltage control voltage source; I: current source; R_{series} is responsible for the instantaneous voltage drop of the step response; $R_{\text{transient}_S}$, $C_{\text{transient}_S}$, $R_{\text{transient}_L}$ and $C_{\text{transient}_L}$ are responsible for short- and long-time constants of the step response

Under normal operating conditions, the instrument performs measurement daily and the pH sensor

requires calibration after the measurement. As discussed above, only 5 min are required to complete fluid displacement, consequently the simulation of the duration during working conditions is set to 15 min and the remainder of the time the instrument is in idle mode. Laboratory tests showed that the voltage (V_{soc}) in the fully discharged state (SOC is 0%) is 11.5 V. Simulation results (Fig. 7) demonstrate that DPM strategy extends battery lifetime by 64.3% (18d, from 28 d to 46 d), which is very close to the calculation results by Eq. (7) (17.8 d, from 28 d to 45.8 d).

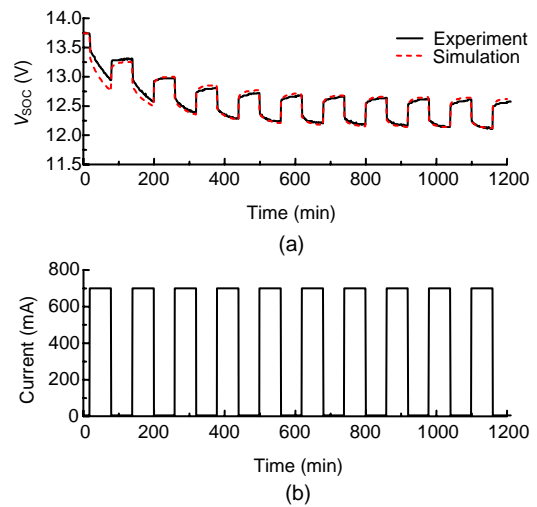


Fig. 6 Comparisons between simulation result and experimental data for 700 mA pulse discharge current. (a) Experimental and simulation V_{SOC} of the battery; (b) Discharge current pulse applied in the experiment and simulation

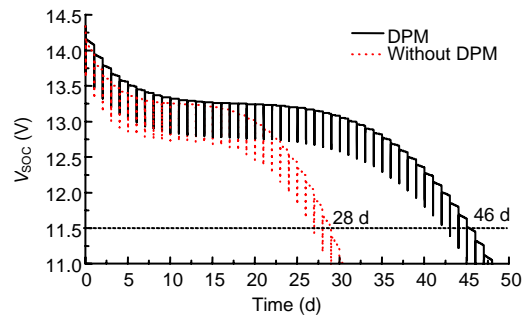


Fig. 7 Simulation results of the battery lifetime

4 Sea trials and results

Sea trials of the auto-calibrating system were performed during the KNOX18RR cruise (Mid-Atlantic Ridge, July–August, 2008, chief scientist

Anna-Louise REYSENBACH, supported by the National Science Foundation of U.S.) on the R/V Roger REVELLE. For deployment, the IrO_x electrode and $\text{Ag}|\text{AgCl}$ electrode were utilized for pH sensors and the signals were collected and recorded by an autonomous real time data-logger (Chen *et al.*, 2005).

An example of the first in situ pH calibration series under deep sea conditions is presented in Fig. 8. In this test, the system was launched on the wire-line into the deep ocean (Aug. 4th, 2008, Fig. 9) to a depth of 3200 m at 26°09' N, 44°52' W in the vicinity of hydrothermal vent Trans-Atlantic Geo-Traversal (TAG, 26° N, Mid-Atlantic Ridge). To compare the data with the laboratory test, each step was set to 20 min. The system operated four functional cycles at this depth. Buffer solutions were prepared according to the same procedure as the laboratory test, and pH (25 °C) of buffer 1 and buffer 2 was measured on-board to be 7.14 and 10.56, respectively. The operational procedure was the same as previously discussed. Between the operational steps, the instrument was in "sleep" mode to save power. By measuring the volume of the buffer reservoirs, the flow rate at depth

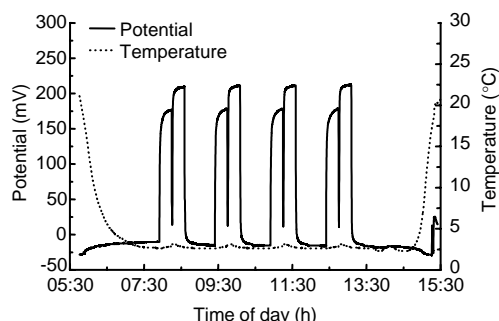


Fig. 8 Measured pH (sensor potential) and temperature recorded at the depth of 3200 m. The trend of temperature curves illustrate the deployment process



Fig. 9 Launching the instrument for seawater pH measurement

was calculated to be 7.5 ml/min, exactly the same as programmed. Fig. 8 shows that the in situ pH data (mV) is in good agreement with the data in Fig. 3, which demonstrates the stability and functionality of the instrument at elevated pressures.

Using the measured potentials of the steady state (collected from 20 readings averaged in the last minute of each step), the calibrated empirical relationship between the measured potential E (mV) and pH value results in the following relationships:

$$E = 674.7 - 65.2\text{pH}. \quad (8)$$

Subsequent analysis and calculation showed that the pH of seawater was 7.62. Data indicated successful performance of in situ standardization and measurement cycles at great depths and high pressures.

5 Conclusions

Long-term in situ monitoring of deep sea aqueous environments is crucial for scientists to understand the geochemical processes of the ocean. The auto-calibrating system has a unique and practical in situ calibration capability, allowing the pH electrode to obtain long-term reliable data. Two methods were used to make sure the instrument worked for periods longer than one month. First, a reduction in the energy loss was achieved through a new mechanical design, and the second, a low power design method was implemented in the electronics design. The simulation and calibration showed that the battery lifetime was extended to 46 d under normal operating conditions. Deep sea trials show that in situ calibration instrument is an effective tool for electrochemical sensors to perform measurement and calibration. This instrument provides a valuable tool which can host electrochemical sensors for pH, H_2 , H_2S , etc., fulfilling most of the principal requirements set by the scientific community.

Acknowledgements

We thank the Jason group and crew members of Roger REVELLE for their dedication and skill during the cruise. Drs. H.C. WU. and W. ZHAO of Zhejiang

University, China are warmly appreciated for their technical support in the mechanical and circuit design of the first prototype.

References

- Benini, L., Bogliolo, A., Micheli, G.D., 2000. A survey of design techniques for system-level dynamic power management. *IEEE Transactions on Very Large Scale Integration (VLSI) Systems*, **8**(3):299-316. [doi:10.1109/92.845896]
- Benini, L., Castelli, G., Macii, A., Scarsi, R., 2001. Battery-driven dynamic power management. *IEEE Design & Test of Computers*, **18**(2):53-60. [doi:10.1109/54.914621]
- Bradley, A.M., Ivey, M.K., Liberatore, S.P., Dueteret, A.R., 1995. Development and testing of thermocouple/thermistor array packages for monitoring temperature at hydrothermal vent sites. *Eos Transactions American Geophysical Union*, **71**:411.
- Chen, C.A., Wang, S.L., Chou, W.C., Sheu, D.D., 2006. Carbonate chemistry and projected future changes in pH and CaCO₃ saturation state of the South China Sea. *Marine Chemistry*, **101**(3-4):277-305. [doi:10.1016/j.marchem.2006.01.007]
- Chen, M., Rincón-Mora, G.A., 2006. Accurate electrical battery model capable of predicting runtime and I-V performance. *IEEE Transactions on Energy Conversion*, **21**(2):504-511. [doi:10.1109/TEC.2006.874229]
- Chen, O.T., Wang, S., Wu, Y., 2003. Minimization of switching activities of partial products for designing low-power multipliers. *IEEE Transactions on Very Large Scale Integration (VLSI) Systems*, **11**(3):418-433. [doi:10.1109/TVLSI.2003.810788]
- Chen, Y., Ye, Y., Yang, C.J., 2005. Integration of real-time chemical sensors for deep sea research. *China Ocean Engineering*, **19**(1):129-137.
- Dickson, A.G., 1993a. The measurement of sea water pH. *Marine Chemistry*, **44**(2-4):131-142. [doi:10.1016/0304-4203(93)90198-W]
- Dickson, A.G., 1993b. pH buffers for sea water media based on the total hydrogen ion concentration scale. *Deep Sea Research Part I: Oceanographic Research Papers*, **40**(1):117-118. [doi:10.1016/0967-0637(93)90055-8]
- Ding, K., Seyfried, W.E.Jr., 2007. In situ measurement of pH and dissolved H₂ in mid-ocean ridge hydrothermal fluids at elevated temperatures and pressures. *Chemical Reviews*, **107**(2):601-622. [doi:10.1021/cr050367s]
- Ding, K., Seyfried, W.E.Jr., Zhang, Z., Tivey, M.K., von Damm, K.L., Bradley, A.M., 2005. The in situ pH of hydrothermal fluids at mid-ocean ridges. *Earth and Planetary Science Letters*, **237**(1-2):167-174. [doi:10.1016/j.epsl.2005.04.041]
- Kumar, A., Bayoumi, M., Elgamel, M., 2004. A methodology for low power scheduling with resources operating at multiple voltages. *Integration*, **37**(1):29-62. [doi:10.1016/j.vlsi.2003.09.005]
- Le Bris, N., Sarradin, P.M., Pennec, S., 2001. A new deep-sea probe for in situ pH measurement in the environment of hydrothermal vent biological communities. *Deep Sea Research Part I: Oceanographic Research Papers*, **48**(8):1941-1951. [doi:10.1016/S0967-0637(00)00112-6]
- Le Bris, N., Sarradin, P.M., Caprais, J.C., 2003. Contrasted sulphide chemistries in the environment of 13° N EPR vent fauna. *Deep Sea Research Part I: Oceanographic Research Papers*, **50**(6):737-747. [doi:10.1016/S0967-0637(03)00051-7]
- Le Bris, N., Zbinden, M., Gaill, F., 2005. Process controlling the physico-chemical micro-environments associated with Pompeii worms. *Deep Sea Research Part I: Oceanographic Research Papers*, **52**(6):1071-1083. [doi:10.1016/j.dsr.2005.01.003]
- Orr, J.C., Fabry, V.J., Aumont, O., Bopp, L., Doney, S.C., Feely, R.A., Gnanadesikan, A., Gruber, N., Ishida, A., Joos, F., et al., 2005. Anthropogenic ocean acidification over the twenty-first century and its impact on calcifying organisms. *Nature*, **437**(7059):681-686. [doi:10.1038/nature04095]
- Pan, Y.W., Seyfried, W.E.Jr., 2008. Experimental and theoretical constraints on pH measurements with an iridium oxide electrode in aqueous fluids from 25 to 175 °C and 25 MPa. *Journal of Solution Chemistry*, **37**(8):1051-1062. [doi:10.1007/s10953-008-9293-z]
- Reimers, C.E., Glud, R.N., 2000. In situ Chemical Sensor Measurements at the Sediment-water Interface. In: Varney, M. (Ed.), *Chemical Sensors in Oceanography*. Gordon and Breach Publishing, Amsterdam, p.249-282.
- Schweighofer, B., Raab, K.M., Brasseur, G., 2003. Modeling of high power automotive batteries by the use of an automated test system. *IEEE Transactions on Instrumentation and Measurement*, **52**(4):1087-1091. [doi:10.1109/TIM.2003.814827]
- Zhao, W., Chen, Y., Yang, C.J., 2009. Design of low-power data logger of deep sea for long-term field observation. *China Ocean Engineering*, **23**(1):133-144.